

## Adaptive Lift Control of an Electrohydraulic Camless Valvetrain System

**Mark D. Anderson**

**Tsu-Chin Tsao**

t-tsao@uiuc.edu

Department of Mechanical and Industrial Engineering

University of Illinois at Urbana-Champaign

Urbana-Champaign, Illinois

**Michael B. Levin**

Scientific Research Laboratory

Ford Motor Company

Dearborn, Michigan

### Abstract

The paper presents an adaptive feedback control of valve lift for an electrohydraulic actuator [1] for camless variable valve timing engine operation. The adaptive control maintains peak value of lift in presence of variations in engine speed, hydraulic fluid temperature and manufacturing variability of valve assemblies.

### System Description

The actuator as shown in figure 1 operates by controlling two solenoid valves for each set of paired engine valves (with four valves per cylinder). During the valve opening, the high-pressure solenoid valve is open, and the net pressure force pushing on the double-acting piston accelerates the engine valve downward. When the solenoid valve closes, pressure above the piston drops, and the piston decelerates pushing the fluid at the lower side back into the high-pressure reservoir.

While the entire valve motion control involves opening, closing, and soft seating control via proper timing and duration of the two solenoid opening pulses, this work considers only the valve lift control. The control objective is to maintain constant peak valve lift from one cycle to another. This is achieved by adjusting the high pressure solenoid pulse width, with longer pulse widths resulting in engine valve lifts.) The open loop tuning of these solenoid pulse variables is quite labor intensive and may change with the environmental conditions and valve units. Adaptive control was deemed necessary for consistent responses and low cyclic variations for changing environmental conditions, different valve units, and valve aging/wears.

### Adaptive Control Scheme

The system drives a pair of valves sharing the same control chamber. Figure 2 shows experimental data of peak lift with respect to solenoid pulse width. The nonlinearity in the curve is due to the transient dynamic relationship between the solenoid pulse width and the solenoid opening area. The dispersed correlation between larger pulse duration and higher lift depicts the deficiency of the hydraulic pump to provide transient high pressure fluid. Therefore, lift under 4 mm was considered in this test. The system has been modeled as a variable gain linear system with a bias offset [3], and takes the form:

$$y(k) = a \cdot u(k-d) + b \quad (1)$$

where the sample time  $k$  is defined as one complete engine cycle, or 720 crank degrees,  $d$  is the combination of sensing and controller-host computer communication delay,  $y$  is the peak lift output,  $u$  is the solenoid valve pulse width, and  $b$  is an offset parameter.

In an ideal case, there should only be sensing delay but no communication delay and hence  $d = 1$ . In this study however, the

serial communications make the delay  $d = 1$  or  $2$  in most cases and maybe more than  $2$  in some cases where the serial communications may not be fast enough for the high engine speed regime.

The reduced-order model was then used to perform a pole-placement design for a feedback controller. The design was performed such that integral control is provided, and a good level of damping is achieved for either case of delay, i.e.  $d = 1$  or  $d = 2$ . The resulting control law is:

$$G_c(z) = \frac{K_c(z-0.05)}{(z-1)(z+0.45)} \quad (2)$$

$$K_c = m/a, \quad (3)$$

,where  $m = 0.287$ , gives similar dominant pole locations.

To estimate the plant parameters, both recursive least squares (RLS) and recursive projection estimation methods were attempted [2]. The experimental results suggested that the RLS method could not maintain a small level of estimation errors consistently as the projection method did. Only the results by projection method are presented here. The model for the estimation was

$$y(k) = \phi^T(k-1)\hat{\theta}(k-1) \quad (4)$$

$$\hat{\theta}(k) = [\hat{a} \ \hat{b}]^T, \quad \phi(k-1) = [u(k-d) \ p]^T \quad (5)$$

The parameter  $p$  is scaled to match the magnitude of  $u(k-d)$ . This scaling was found necessary to ensure equal adaptation of both parameters. The projection adaptation algorithm with fixed dead zone is

$$e(k) = y(k) - \phi^T(k-1)\hat{\theta}(k-1)$$

$$\text{if } |e| \leq \delta, e = 0, \text{ else } e = e - \delta \cdot \text{sign}(e)$$

$$\hat{\theta}(k) = \hat{\theta}(k-1) + \frac{\alpha \cdot \phi(k-1)e(k)}{c + \phi^T(k-1)\phi(k-1)} \quad (6)$$

### Experimental Results

In the adaptive control experiment, the tests underwent a scheduled cycle of lift and engine speed changes. The two parameters for the projection estimation method: the adaptation gain  $\alpha$ , and the dead zone  $\delta$  were tuned first. Each parameter is chosen with the goal being minimization of output estimation error, defined on a rms. basis:

$$e_{rms} = \sqrt{\frac{\sum_i (y_i - \hat{y}_i)^2}{i}} \quad (7)$$

A range of  $k$  from 0.01 to 1.9 was tested, and the estimation error for each case is shown vs.  $k$  in figure 3. A value of 1.0 was chosen as it had the lowest error out of the values tested. With the error gain and offset scale fixed, the dead zone choice was optimized. A range of dead zones from 0.01 to 0.85 mm was tested; the resulting estimation errors are shown vs. dead zone choice in figure 4. A dead zone too low may cause excessive oscillation. It is apparent that estimation error does decrease slightly when the dead zone is decreased below approximately 0.0075 mm. Therefore, this value was chosen for the dead zone.

Figure 5 demonstrates the ability of the adaptive lift control to track the variability due to temperature change. The steady state values of the real-time estimated valve parameters and the pulse width to generate a constant lift are shown in terms of the fluid temperature. As expected, the higher temperature has lower fluid viscosity and hence requires smaller pulse width to achieve the same lift.

Figure 6 demonstrates the ability of adaptive control to maintain consistent performance of two different valves, where the different valve gains and offsets were identified by the adaptive scheme as shown. The transient lift responses of the two cases have been maintained consistently as shown in the top plot, indicating proper functioning of the adaptive control.

**References**

- [1] Schechter M. and Levin M. "Camless Engine," SAE paper 960581.
- [2] Anderson, M.A., "Adaptive Control of a Camless Electrohydraulic Valvetrain" M.S. Thesis, University of Illinois at Urbana-Champaign, 1997.

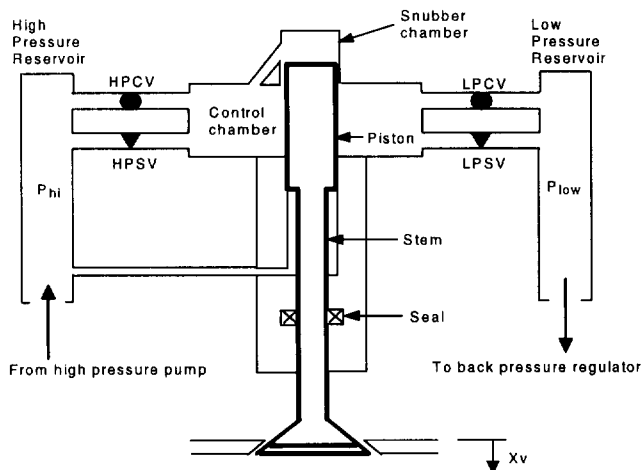


Figure 1 Actuator Schematic Diagram

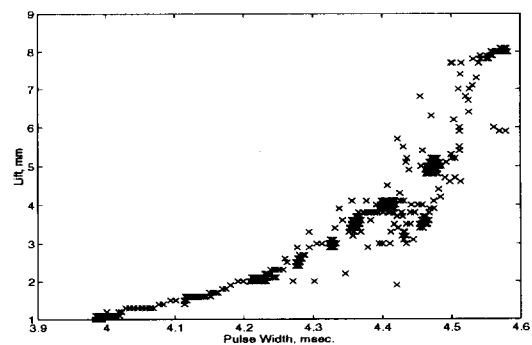


Figure 2 Lift Vs. Pulse Width

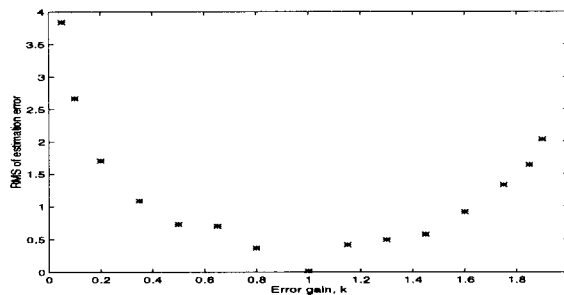


Figure 3. RMS value of estimation error vs. error gain.

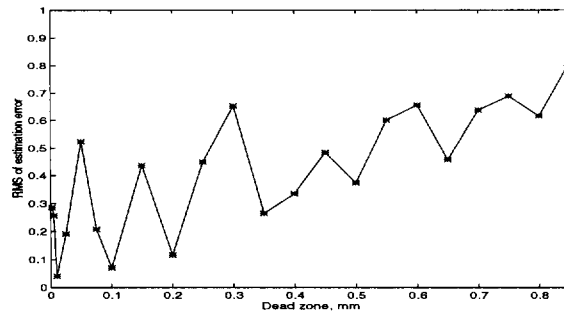


Figure 4. RMS value of estimation error vs. dead zone.

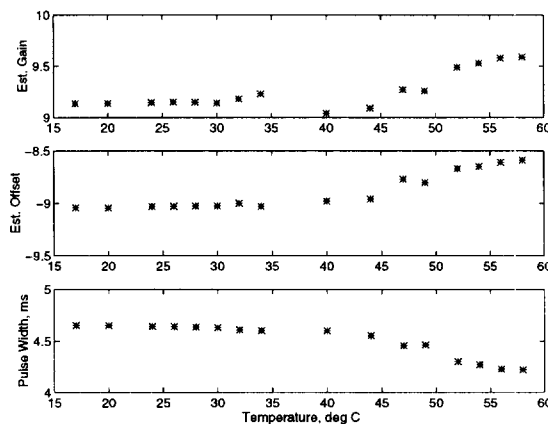


Figure 5. Steady-state pulse width and  $\theta$  vs. temperature at 1.8mm/1000 RPM.

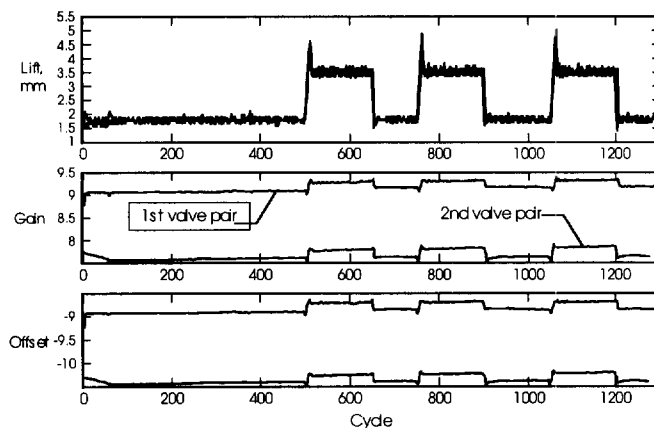


Figure 6. Lift Response and Parameter Estimation for two Different Valves